

Arctic Ocean Ventilation Studied with a Suite of Anthropogenic Halocarbon Tracers

M. KRYSSELL AND D. W. R. WALLACE

The chlorofluoromethanes (CFMs: CCl_2F_2 and CCl_3F), methyl chloroform (CH_3CCl_3), and carbon tetrachloride (CCl_4) have been measured in deep waters of the Arctic Ocean. Oceanic and atmospheric inventories of these compounds result from known anthropogenic releases; because the CFMs and CCl_4 are also chemically nonreactive, they can be used as transient tracers of ocean circulation. The input history of CCl_4 is longer than that of any other transient tracer identified to date (~ 70 years). This long input history, together with an e -folding time scale of increase (τ) of ~ 28 years, makes CCl_4 potentially the most useful tracer for calibrating models of the oceanic uptake of the fossil-fuel CO_2 transient ($\tau \approx 25$ years). The bottom water of the Nansen Basin, Arctic Ocean, has detectable CCl_4 but undetectable CFMs and CH_3CCl_3 , which suggests either that the bottom water is ~ 50 years old, or that there is a small, nonanthropogenic component of atmospheric CCl_4 (< 6 parts per trillion by volume).

THE CHLOROFUOROMETHANES (CFMs) or Freons (F-11, CCl_3F , and F-12, CCl_2F_2) are being studied throughout the world's oceans (1-3) because they can be used to infer rates of subsurface circulation and mixing. Analogous studies with bomb-derived tracers (^3H and ^{14}C) are the basis for calibrating models of anthropogenic CO_2 uptake by the oceans (4). The CFMs are useful transient tracers because of their time-dependent input into the surface layers of the ocean (which correspond to temporal increases in their atmospheric concentrations) and because they are chemically nonreactive. Methyl chloroform (1,1,1-trichloroethane, CH_3CCl_3) and carbon tetrachloride (CCl_4) have also been released to the environment in large amounts as a result of man's activities. We measured the distributions of these anthropogenic halocarbons in the Arctic Ocean to investigate processes of exchange between near-surface and deep waters (5-7). The data were collected during the Arktis IV/3 cruise of the research vessel *Polarstern* across the Nansen Basin, Arctic Ocean, during July and August 1987.

The historical tracer input functions need to be characterized so that rates of ocean ventilation can be inferred from tracer distributions. We estimated Arctic Ocean surface water concentrations through time for CCl_4 ,

CH_3CCl_3 , and the CFMs (Fig. 1A), using anthropogenic release estimates and the mean atmospheric lifetimes of these compounds (7-10) for the period before high-quality atmospheric measurements were made. The lifetime estimates that we used

were 52 years for CCl_4 , 6.3 years for CH_3CCl_3 , 74 years for F-11, and 111 years for F-12. The resulting estimates of cumulative atmospheric inventories have been normalized to concentrations (expressed as dry air mixing ratios) measured in remote regions of the Northern Hemisphere in 1975, when reliable measurements began to be made (11). Atmospheric histories for more recent years are based on direct measurements (11); in January 1985, for example, Northern Hemisphere levels were 130 parts per trillion (10^{12}) by volume (pptv) CCl_4 , 158 pptv CH_3CCl_3 , 217 pptv F-11, and 394 pptv F-12. We calculated Arctic Ocean surface water concentrations using these atmospheric mixing ratio histories and published solubility data (12); hence the calculated concentrations (Fig. 1A) represent 100% saturation with respect to contemporary atmospheric levels of the various compounds (13).

Several different scenarios for the past release of CCl_4 have been suggested (10, 14, 15), but the differences among these scenarios are less when cumulative atmospheric inventories normalized to direct measurements are considered. We assume that preindustrial levels of all compounds were zero, although natural sources of CCl_4 have been postulated (16). Most researchers have concluded that preindustrial levels were negligible (17), but a small natural background

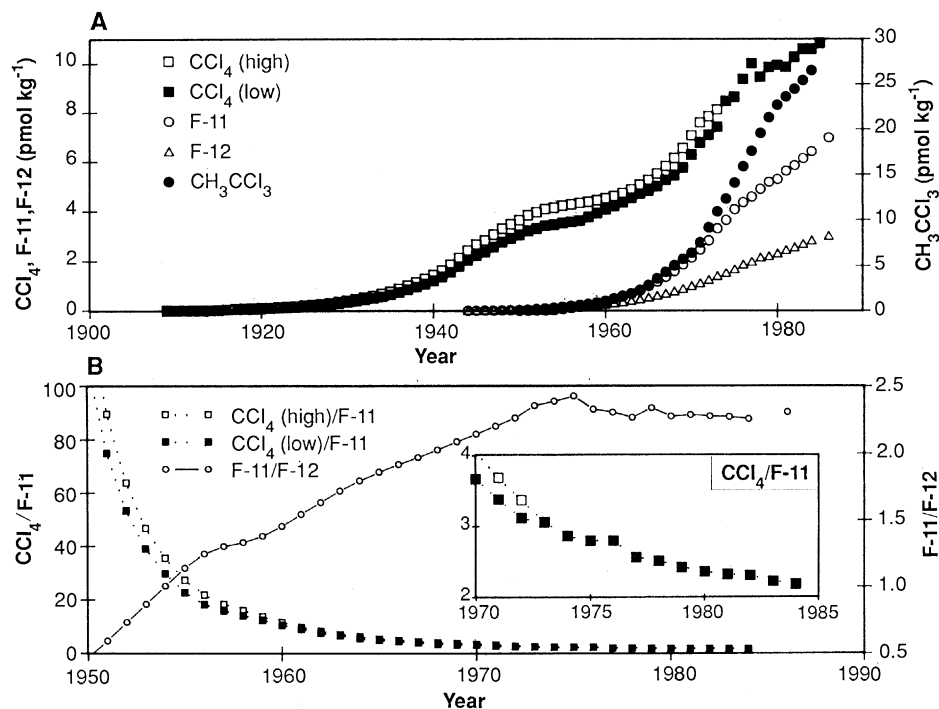


Fig. 1. (A) Estimates of Arctic Ocean surface water halocarbon concentrations through time based on reconstructed atmospheric mixing ratios and gas solubility data for seawater at -1°C with a salinity of 35 practical salinity units (psu). The separate scale for the more soluble CH_3CCl_3 is on the right. Two curves are presented for CCl_4 , on the basis of upper- and lower-bound anthropogenic release scenarios (10). (B) Temporal trends of halocarbon ratios in Arctic Ocean near-surface water. The inset displays the recent trend of $\text{CCl}_4/\text{F-11}$ on an expanded scale.

M. Krysell, Department of Analytical and Marine Chemistry, Chalmers University of Technology and University of Göteborg, S-412 96, Göteborg, Sweden.
D. W. R. Wallace, Oceanographic Sciences Division, Brookhaven National Laboratory, Upton, NY 11973.

level cannot be ruled out.

The input history for CCl_4 is 30 to 40 years longer (Fig. 1A) than that of any other transient tracer (for example, CFMs, ^3H , or bomb ^{14}C) because of widespread dispersive use of CCl_4 in the United States from 1908 through the 1950s. Realization of the toxicological effects of CCl_4 led to the substitution of safer chemicals for uses such as dry-cleaning, industrial solvents, and fumigation. CCl_4 is now produced primarily as a chemical feedstock for chlorofluoromethane production. The long input history for CCl_4 , together with its e -folding time scale of ~ 28 years, which is similar to that of the fossil fuel CO_2 transient (~ 25 years), implies that measurements of CCl_4 levels in the oceans can be used to refine estimates of the amount of anthropogenic CO_2 taken up by the oceans. In contrast, the characteristic time scales of input of other transient tracers are much less than that of fossil-fuel CO_2 , which began to be input in the last century; therefore, extrapolation of the transient tracer-calibrated CO_2 uptake models was required. The use of CCl_4 should significantly reduce this extrapolation.

The halocarbon ratios, F-11/F-12 and F-11/ CCl_4 , in Arctic Ocean surface waters through time (Fig. 1B) provide a means to date water masses. In applying this technique, a water mass that sinks below the surface layer (where it is in close contact with the atmosphere) is assumed to preserve an anthropogenic halocarbon ratio that is a function of the contemporary atmospheric ratio and the solubility of the compounds of

interest. Hence for tracer pairs whose atmospheric ratios have changed with time, the observed ratio in a water mass can be related to the year that the water mass left the surface (that is, its "age"). Although mixing can complicate this relation, F-11/F-12 has given useful indications of deep ocean circulation rates (1). Figure 1B shows that F-11/ CCl_4 has changed much more dramatically with time than F-11/F-12 and therefore may be a better tracer. For the period 1975 to 1985, F-11/F-12 has remained almost constant and consequently cannot be used to date recently formed water masses, while F-11/ CCl_4 has decreased from ~ 3 to ~ 2 (Fig. 1B) and therefore can be used. Another anthropogenic halocarbon ($\text{CCl}_2\text{FCClF}_2$, F-113) has recently been shown to be a useful transient tracer for the period since 1977 (18). Thus, the concentrations of CCl_4 , together with F-11, F-12, and F-113, can provide information concerning ocean ventilation time scales ranging from 1 to 70 years.

The concentrations of CFMs, CCl_4 , and CH_3CCl_3 at station 358 in the central Nansen Basin share similar depth profiles throughout the upper 1000 m of the water column (Fig. 2A). The variations reflect the degree of contact that each layer of water has with the atmosphere, that is, its rate of ventilation. Clearly this structure could not have developed from simple vertical mixing; rather it reflects the importance of ventilation along constant density surfaces from regions where these surfaces intersect the ocean surface.

Through the upper 350 m of the water column, F-11/F-12 (Fig. 2B) remains essentially constant at $2.26 (\pm 0.05)$. This is the expected value for water that has been ventilated during most of the years 1972 through 1987 [with gas solubilities calculated for appropriate temperature ($\sim 0^\circ\text{C}$) and salinity (~ 34.4 practical salinity units)]. Similarly, $\text{CCl}_4/\text{F-11}$ also stays essentially constant with depth, with a value of $2.26 (\pm 0.28)$, which corresponds to the expected value for the period 1975 through 1980. Below 350 m, the variation in $\text{CCl}_4/\text{F-11}$ with depth (2 to 30) is much larger than the variation in F-11/F-12 (2.3 to 1.2). These data show that despite our less precise measurement of $\text{CCl}_4/\text{F-11}$, this ratio provides better age resolution than does F-11/F-12 at both short (< 15 years) and long time scales. Assignment of water mass ages on the basis of the two ratios gives comparable results. For example, at 1000 m the F-11/F-12 age is 22 to 23 years and the $\text{CCl}_4/\text{F-11}$ age is 24 to 25 years. At 2000 m, the ages are 26 to 27 and 30 years, respectively (19). Below 3000 m, $\text{CCl}_4/\text{F-11}$ tends to infinity because F-11 becomes undetectable.

In the bottom water (> 3000 m), the CFMs and CH_3CCl_3 fall below their respective detection limits ($0.01 \text{ pmol kg}^{-1}$ for the CFMs, 0.4 pmol kg^{-1} for CH_3CCl_3). Hence the bottom water has less than 1/500 the concentration of F-11 and less than about 1/300 the concentration of CH_3CCl_3 and F-12 as near-surface water. In contrast, CCl_4 levels in the bottom water are only about 1/20 the concentration in near-surface wa-

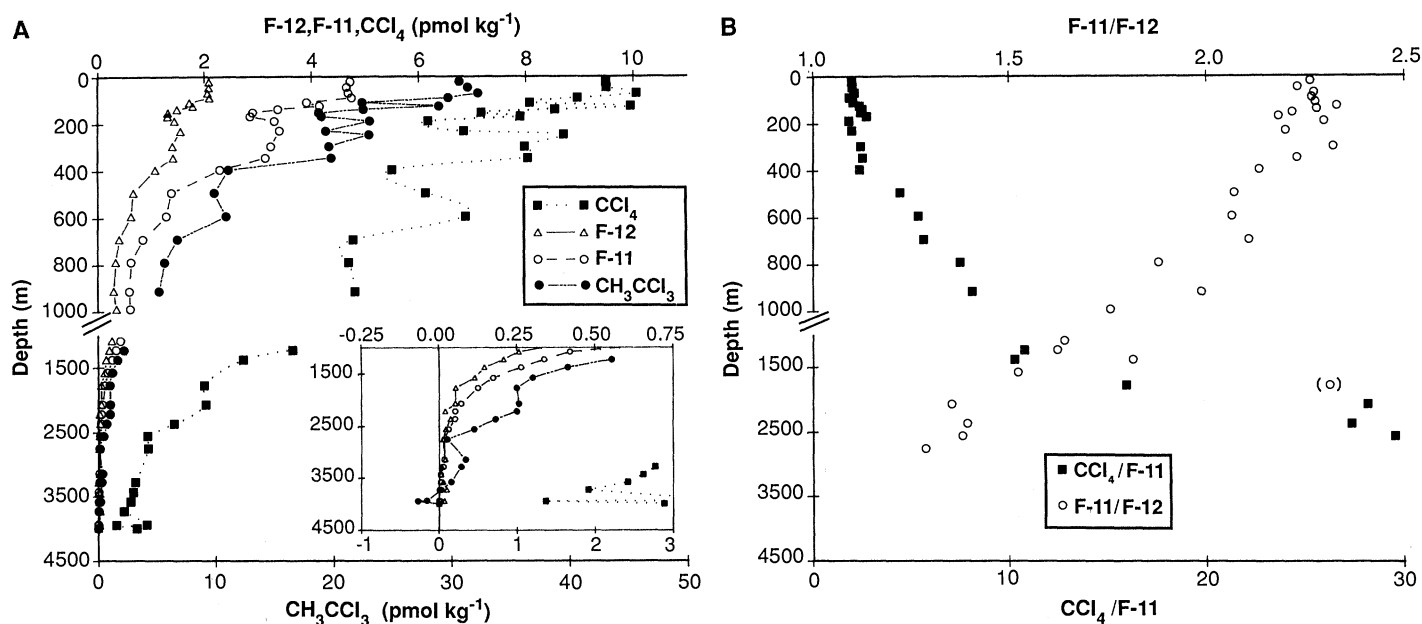


Fig. 2. Depth profiles from station 358 in the central Nansen Basin, Arctic Ocean ($84^\circ 01' \text{N}$, $30^\circ 33' \text{E}$); the depth scale changes below 1000 m. (A) Halocarbon concentration profiles. The inset shows deep distributions on expanded scales; negative concentrations arise from variability in the analyti-

cal blanks that have been subtracted from the measured values. (B) Halocarbon ratio profiles; the ratios are indeterminate below ~ 3000 m because F-11 is below the analytical detection limit.

Table 1. Amount of various halocarbon compounds that can be transported downward in the Arctic Ocean (T) with the particulate organic carbon flux (F_p). Resulting bottom water concentrations are given in the last column (c_{wp}).

Compound	n (years)	c_w ($g\ g^{-1}$)	F_p ($g\ m^{-2}$ $year^{-1}$)	K_p	T ($g\ m^{-2}$)	c_{wp} ($pmol\ kg^{-1}$)
CCl_4	67	6.5×10^{-13}	1*	570†	5×10^{-8}	3×10^{-4}
F-11	34	1.6×10^{-13}	1*	385‡	4×10^{-9}	3×10^{-5}
F-12	41	6.4×10^{-14}	1*	216‡	1×10^{-9}	9×10^{-6}
CH_3CCl_3	30	1.4×10^{-12}	1*	427‡	4×10^{-8}	3×10^{-4}

*Total primary production in the Central Arctic Ocean is $<1\ g\ m^{-2}\ year^{-1}$. Of this only a very small fraction would reach the bottom water. Hence this is a large overestimate of the POC flux at depth. †Measured (21). ‡Estimated (from relation with octanol-water partition coefficient) (21).

ters and are well above the detection limit of $0.1\ pmol\ kg^{-1}$. In our measurements, we were careful to check for possible sample contamination (20).

Of concern is whether the downward flux of particulate organic matter in the oceans can transport appreciable amounts of hydrophobic CCl_4 . We have estimated the integrated particulate transport of the four compounds discussed in this report, using the expression

$$T = 2\ n\ c_w\ F_p\ K_p$$

where T is the time-integrated transport of the compounds via the particulate flux, n is the number of years that the compound has been above detection limit in the ocean, c_w is the time-averaged surface water concentration (in grams per gram) during this period, F_p is the particulate organic carbon (POC) flux (in grams per square meter per year), and K_p is a bioaccumulation factor defined on a dry weight basis (21). The factor of 2 is needed to convert grams of POC to grams dry weight. Bottom water concentrations (c_{wp}) are calculated with the assumption that all of the transported compound returns to the dissolved phase in the deepest 1000 m of the water column.

For parameter values and assumptions that greatly exaggerate the significance of this transport pathway, the resulting bottom water concentrations are all several orders of magnitude below the detection limits (Table 1). Therefore none of these compounds should be significantly affected by open ocean particulate transport.

Another potential loss mechanism for these compounds is hydrolysis (or dehydrohalogenation for CH_3CCl_3). Hydrolysis lifetimes for CCl_4 in the ocean are much greater than 7000 years (22). Lifetimes for the CFMs should be even longer. Clearly hydrolysis is not a significant sink for these compounds. Hydrolysis and dehydrohalogenation are significant for CH_3CCl_3 , however, which has a lifetime (23) of ~ 0.75 years in seawater at $10^\circ C$ (its lifetime in cold Arctic waters is considerably longer). Consequently, it is safe to regard the CFMs and

CCl_4 as conservative tracers of water movement over a hundred-year time scale at least, whereas CH_3CCl_3 is subject to chemical degradation at a rate that limits its utility as a tracer.

The observation that the CFMs and CH_3CCl_3 are undetectable in the central Nansen Basin bottom water whereas CCl_4 is detectable suggests that this water mass might have an age that corresponds to the first half of the 20th century when anthropogenic CCl_4 was present in the environment, but CFMs and CH_3CCl_3 were absent. The lowest CCl_4 concentration measured ($\sim 0.5\ pmol\ kg^{-1}$) corresponds to a level that would have been expected in surface waters during the mid-1930s, which suggests that the age of the water is ~ 50 years. This falls within the age range of 10 to 100 years that has been suggested on the basis of limited 3H and ^{14}C data collected from the basin periphery (24). The concentration of ^{14}C in samples collected during the Arktis IV/3 cruise, however (25), indicates that the bottom water might be considerably older than 50 years. The only alternative explanation is that there is a natural preindustrial background of less than or equal to 6 pptv CCl_4 . Natural sources of CCl_4 have been postulated by several researchers (16). Analyses of older ocean waters (for example, North Pacific deep water) or, preferably, of air trapped in ice cores, will be required to determine whether the preindustrial background of CCl_4 is significant.

REFERENCES AND NOTES

- R. F. Weiss, J. L. Bullister, R. H. Gammon, M. J. Warner, *Nature* **314**, 608 (1985).
- R. H. Gammon, J. Cline, D. Wisegarver, *J. Geophys. Res.* **87**, 9441 (1982).
- J. L. Bullister and R. F. Weiss, *Science* **221**, 265 (1983); D. W. R. Wallace and J. R. N. Lazier, *Nature* **332**, 61 (1988).
- W. S. Broecker, T.-H. Peng, R. Engh, *Radiocarbon* **22**, 565 (1980); U. Siegenthaler, *J. Geophys. Res.* **88**, 3599 (1983); T.-H. Peng, *Radiocarbon* **28**, 363 (1986).
- H. B. Singh, L. J. Salas, R. E. Stiles [*J. Geophys. Res.* **88**, 3675 (1983)] have reported surface water concentrations of CFMs and CCl_4 ; E. Fogelqvist [*ibid.* **90**, 9181 (1985)] has reported concentrations of CCl_4 , CH_3CCl_3 , CCl_2CCl_2 , and $CHBr_3$ to 2500 m in Fram Strait, but she did not measure the CFMs.

- We analyzed for CCl_4 and CH_3CCl_3 with a Hewlett-Packard 5890 gas chromatograph (GC) and electron capture detector (ECD), equipped with an SE-54 capillary column (50 m by 0.32 mm in inside diameter, 0.15- μm film); carrier gas was helium; the ECD make-up gas was nitrogen. Water samples were extracted with pentane (pentane to water phase ratio of 1/128). Standard solutions were prepared by an additional two stages of serial dilution with a microsyringe from stock solutions that were gravimetrically prepared in pentane. The pentane contained $CBrCl_3$ as an internal standard. Pentane extract (25 μl) was injected directly on-column via a rotary valve. The GC was temperature-programmed from 40° to $85^\circ C$ at $7^\circ C$ per minute. The CFM analyses were performed on a Varian 3300 GC with ECD, with purge-and-trap techniques similar to those described by D. W. R. Wallace and R. M. Moore [*J. Geophys. Res.* **90**, 1155 (1985)]. Total analytical precision for near-surface samples was $\sim 10\%$ for CCl_4 and CH_3CCl_3 , 2.5% for F-12, and 4% for F-11. The CFM values are reported relative to the Scripps Institution of Oceanography 1986 calibration scale (R. F. Weiss, personal communication). Atmospheric concentrations of CCl_4 and CH_3CCl_3 are expressed relative to the Atmospheric Lifetime Experiment-Global Atmospheric Gases Experiment (ALE-GAGE) scale [R. A. Rasmussen and J. E. Lovelock, *J. Geophys. Res.* **88**, 8369 (1983); R. A. Rasmussen and M. A. K. Khalil, *Chemosphere* **13**, 789 (1984); (7)]. Our seawater data for CCl_4 and CH_3CCl_3 are based on our own calibration and have not been intercalibrated with the ALE-GAGE scale.
- R. Prinn *et al.*, *Science* **238**, 945 (1987).
- Chemical Manufacturers Association, Fluorocarbon Program Panel (FPP), *World Production and Release of Chlorofluorocarbons 11 and 12 Through 1981*, FPP Report 83-F (Chemical Manufacturers Association, Washington, DC, 1983).
- D. M. Cunnold *et al.*, *J. Geophys. Res.* **91**, 10797 (1986).
- P. G. Simmonds *et al.*, *ibid.* **88**, 8427 (1983).
- R. A. Rasmussen and M. A. K. Khalil, *Science* **232**, 1623 (1986).
- M. J. Warner and R. F. Weiss, *Deep Sea Res.* **32**, 1485 (1985); R. J. Hunter-Smith, P. W. Balls, P. S. Liss, *Tellus* **35B**, 170 (1983).
- Our measurements indicate that these ice-covered surface waters are significantly undersaturated in these compounds [65% saturation for F-12 and 63% saturation for F-11 at 20 m depth, relative to our measured atmospheric mixing ratios of 442 pptv (F-12) and 247 pptv (F-11)]. Therefore, historical trends are represented adequately in Fig. 2, but surface water concentrations are undoubtedly overestimated.
- I. E. Galbally, *Science* **193**, 573 (1976).
- H. B. Singh *et al.*, *ibid.* **192**, 1231 (1976).
- J. E. Lovelock, R. J. Maggs, R. J. Wade, *Nature* **241**, 194 (1973); W. Fencal, *Science* **215**, 923 (1982).
- A. P. Altschuller, *Environ. Sci. Technol.* **10**, 596 (1976); W. B. Neely, *Sci. Total Environ.* **8**, 267 (1977); V. Ramanathan, R. J. Cicerone, H. B. Singh, J. T. Kiehl, *J. Geophys. Res.* **90**, 5547 (1985); T. E. Graedel and D. L. Allara, *Atmos. Environ.* **10**, 385 (1976).
- D. P. Wisegarver and R. H. Gammon, *Geophys. Res. Lett.* **15**, 188 (1988).
- Ratio-based ages with CCl_4 are approximate because the seawater data have not been directly intercalibrated with the atmospheric data, which define the source function (6). The small difference between the F-11/F-12 and CCl_4 /F-11 ages might result from a variety of causes including analytical and calibration error, invalid assumptions of the ratio-dating method, and the presence of a small nonanthropogenic component of CCl_4 .
- Seven sampling bottles were closed at the same depth in deep water that had low halocarbon concentrations. The bottles were kept sealed until sampled. Samples were collected hourly (0 to 6 hours after being brought on deck) and analyzed for halocarbons. The concentrations of all analyzed species remained essentially constant over time. Liquid-liquid extraction with pentane was carried out eight

(±10%) that matched the pentane blank within 10%. The background for CH₃CCl₃ was 3.3 pmol kg⁻¹ (±5%). All samples were corrected for these backgrounds. The CH₃CCl₃ and CCl₄ concentrations in samples stored overnight in the extraction bottles were the same as the concentrations analyzed immediately after collection. Bottom water CH₃CCl₃ levels were below the detection limit even though CH₃CCl₃ is the most soluble of the compounds measured; these data indicate that contamination during sampling was negligible.

21. H. Geyer *et al.*, *Chemosphere* **13**, 269 (1984). We assume that estimated or measured bioaccumulation

factors for the freshwater alga *Chlorella fusca* are roughly appropriate for partitioning of halocarbons between seawater and marine organic matter. The bioaccumulation factor is defined as

$$K_p = \frac{[\text{concentration in } Chlorella \text{ (gram per gram dry weight)}]}{[\text{concentration in water (gram per gram)}]}$$

22. I. Fells and E. A. Moelwyn-Hughes, *J. Chem. Soc.* **1959**, 398 (1959); W. Mabey and T. Mill, *J. Phys. Chem. Ref. Data* **7**, 383 (1978).
23. C. R. Pearson and G. McConnell, *Proc. R. Soc. London Ser. B* **189**, 305 (1975).

London Ser. B **189**, 305 (1975).

24. H. G. Ostlund *et al.*, *J. Geophys. Res.* **92**, 3769 (1987).
25. L. G. Anderson *et al.*, *Deep Sea Res.*, in press.
26. The officers, crew, and scientific staff of R.V. *Polarstern* provided support and cooperation; we particularly thank L. Anderson, E. P. Jones, K. P. Koltermann, B. Kromer, P. Schlosser, J. Swift, J. Thiede, and F. Zemlyak. A gas chromatograph was provided by E. Fogelqvist. D.W. was supported by Department of Fisheries and Oceans, Government of Canada, during the data collection phase of this project.

10 May 1988; accepted 2 September 1988

Thermodynamic Efficiency of Brittle Frictional Mountain Building

TERENCE D. BARR AND F. A. DAHLEN

An active fold-and-thrust belt in unchanging tectonic and climatic conditions attains a dynamic steady-state in which the influx of accreted material at the toe is balanced by the erosive efflux off the top. The overall balance of energy in such a steady-state fold-and-thrust belt is described by the equation $\dot{E} = \dot{W}_G + Q$, where \dot{E} is the rate at which both mechanical and heat energy are added from external sources, \dot{W}_G is the rate of work performed against gravitational body forces, and Q is the rate at which waste heat flows out of the upper and lower boundaries. The total amount of power being supplied to the active Taiwan fold-and-thrust belt by the subducting Eurasian plate and in situ radioactivity is 4.2 gigawatts. Because only 0.5 gigawatts are expended in doing useful work against gravity and the remaining 3.7 gigawatts are ejected as heat, the efficiency of brittle frictional mountain building in Taiwan is 11 percent.

FOLD-AND-THRUST BELTS ALONG THE margins of many compressive plate boundaries are one of the more visible surface manifestations of the thermal convection in the earth's interior. The principal source of the energy that drives the deformation and uplift in a fold-and-thrust belt is the mechanical work performed on it by the underlying subducting slab. The heat content of the rocks accreted at the toe and in situ radioactivity are additional energy sources. Most of the incoming energy is dissipated against friction and then is ejected as waste heat out of the upper and lower boundaries; uplifting rocks against gravity is the only useful work performed in a fold-and-thrust belt. In this report, we analyze the gross thermodynamic efficiency of this process, using the active fold-and-thrust belt in Taiwan as an example. The regional structure and pore-fluid pressures in the Taiwan fold-and-thrust belt are well determined from data acquired during petroleum exploration (1, 2), and this makes it an ideal laboratory for studying brittle frictional mountain building.

Active deformation in an idealized fold-and-thrust belt (Fig. 1) is confined to a trapezoidal segment of a wedge overlying a planar décollement fault. For simplicity, we

Department of Geological and Geophysical Sciences, Princeton University, Princeton, NJ 08544.

assume that the taper of the wedge is small, that is, $\alpha + \beta < 1$, where α is the constant surface slope and β is the constant dip of the basal décollement fault (in radians). The thin end of the wedge is the toe or deformation front, where an undeformed sedimentary section of thickness h is being accreted, and the thick end is the backstop of the fold-and-thrust belt, where deformation ceases. We use a Cartesian coordinate system with x aligned along the top surface of the wedge and z pointing obliquely down. The origin is located at the vertex of the wedge so that the distance to the deformation front is $x_0 = h(\alpha + \beta)^{-1}$. The steady-state width W is determined by the flux-balance condition $hV = \dot{e}W$, where V is the downdip subduction velocity of the rigid lower plate and \dot{e} is the uniform erosion rate.

The coefficient of internal friction of the rocks in the wedge is denoted by $\mu = \tan \phi$ (ϕ is given by the failure envelope of the rocks in the wedge); μ_b is the coefficient of friction along the base, and λ and λ_b are the pore-fluid to lithostatic pressure ratios in the wedge and on the base; we regard all four of these strength parameters as constant. A critically tapered fold-and-thrust belt is one on the verge of Coulomb failure everywhere; the greatest and least principal stresses in a thin-skinned, critically tapered wedge are (3) $\sigma_{xx} = \sigma_1 = -\Lambda \rho g z$ and $\sigma_{zz} = \sigma_3$

$= -\rho g z$, where ρ is the constant rock density and $\Lambda = 1 + 2(1 - \lambda)\sin \phi / (1 - \sin \phi)$. With a simple mass balance argument (4), the x and z components of the steady Eulerian velocity of rocks relative to the backstop are found to be

$$u = [-\dot{e} + hVx^{-1}(1 + x_0/W)]/[\alpha + \beta]$$

and

$$v = -\dot{e} + hVzx^{-2}(1 + x_0/W)/(\alpha + \beta)$$

The volumetric rate at which energy is dissipated against internal friction in the wedge is

$$\sigma_1 \dot{\epsilon}_1 + \sigma_3 \dot{\epsilon}_3 = (\Lambda - 1)\rho g x_0 (1 + x_0/W)Vzx^{-2}$$

where $\dot{\epsilon}_1 = \partial u / \partial x$ and $\dot{\epsilon}_3 = \partial v / \partial z$ are the principal strain rates, and the rate of frictional dissipation on the basal décollement fault is

$$\tau_b(V - u) = \mu_b(1 - \lambda_b)\rho g H V W^{-1}(x - x_0)$$

We ignore any surface energy required to create fresh fractures in the wedge and assume that all the dissipated energy is manifested as heat.

Dahlen (4) showed that the balance of mechanical energy in a thin-skinned fold-and-thrust belt can be described by the equation

$$\dot{W}'_B = \dot{W}'_G + H_S + H_D$$

where

$$\dot{W}'_B = -V \int_B \sigma_1 dz$$

$$\dot{W}'_G = \rho g \int_C (u\alpha - v + V\beta) dx dz$$

$$H_S = \int_C (\sigma_1 \dot{\epsilon}_1 + \sigma_3 \dot{\epsilon}_3) dx dz$$

$$H_D = \int_D \tau_b(V - u) dx$$

Here C denotes the wedge cross section, and F , T , B , and D denote the front, top, back, and décollement surfaces. In this form, the quantity \dot{W}'_B is the rate of work performed on the back of the wedge by the backstop, and \dot{W}'_G is the rate of work performed against gravitational body forces in the reference frame attached to the subduct-